Application of Laser Array Spots Thermography for 3D Surface Topography and Defect Detection

By Na Yan*, Kang Tian*, Qian Zhang*, Jianping Peng* and Jinlong Lee*

* School of Physical Science and Technology, Southwest Jiaotong University, Chengdu, PR China, *adams.peng@swjtu.edu.cn*

Abstract

Laser array spots thermography is a novel non-contact non-destructive testing (NDT) technique that offers rapid detection and intuitive results. However, industrial metal components typically possess complex geometries, creating significant challenges for precise detection and subsequent processing of temperature data sequences. In this paper, we analyze the laser array spots thermography process and propose a method that utilizes a single set of detection data to simultaneously reconstruct the three-dimensional surface topography of complex shapes and perform defect detection. By examining the influence of complicated surface geometries on thermal NDT methods, this approach enhances the localization accuracy and reliability of defect detection.

1. Introduction

Non-destructive testing (NDT) refers to the evaluation of an object's physical condition through various methods and techniques without damaging or interfering with its functionality, in order to understand its characteristics and subsequent behavior [1]. As such, it plays a critical role in ensuring the safety of engineering structures, assessing material properties, and monitoring manufacturing quality. Among the various NDT methods, infrared thermography (IRT) has gained widespread application and rapid development in recent years due to its non-contact, fast, and full-field measurement characteristics [2]. Thermal imaging technology detects subtle temperature distribution differences (thermal maps) on an object's surface caused by internal structures or defects, and inversely reconstructs its internal state information. This technology has significant defect detection capabilities for internal delamination, layering, cracks, inclusions, corrosion, and damage to composite material structures. It is widely applied in fields such as aerospace, energy and power, civil construction, electronics manufacturing, and cultural heritage preservation.

In the field of industrial non-destructive testing, traditional two-dimensional thermal imaging technology is limited by the planar projection mechanism, making it difficult to adapt to complex curved structures. Additionally, it is prone to geometric distortions that can obscure true defect signals [3]. Three-dimensional thermal imaging technology, through specific technical means, not only captures the surface temperature information of an object but also integrates the object's three-dimensional morphological data to construct a temperature field distribution with spatial depth coordinates. However, early 3-D thermal imaging technology simply integrated additional 3-D geometric data measurement systems into existing passive thermal imaging systems, resulting in issues such as the need for complex cross-modal image registration algorithms. In active thermal imaging, 3-D information and temperature sequences are usually fused through complex image registration techniques [4], but they are still obtained separately, failing to unify the mathematical models for 3-D reconstruction and thermal imaging detection. Therefore, research that uses a single heat source while ensuring high-precision three-dimensional reconstruction and accurate defect detection is of great significance.

Özer [5] proposed a novel three-dimensional Mesh Infrared Thermography (3D MIT) technique. By suspending an array of copper spheres in the airflow and recording the scene with an infrared camera, they reconstructed the 3-D temperature field of an otherwise transparent gas (air). The mesh minimizes flow disturbance and parasitic heat-conduction errors, thereby increasing measurement accuracy; validation against thermocouple readings and particle-image velocimetry (PIV) confirmed the method's reliability. Heifetz [6] developed a thermal-tomography-based 3-D imaging framework for detecting subsurface defects in additively manufactured (AM) metal parts. Their approach reconstructs volumetric temperature distributions from transient surface data, enabling non-destructive localization of hidden flaws within metallic AM components. Chen [7] Introduced a 3-D reconstruction scheme that fuses infrared thermography with visual-hull intersection. Multi-view 2-D thermal and RGB images are acquired, segmented automatically via Otsu and entropy thresholds, and registered through camera calibration. The resulting model yields a 3-D temperature map of internal heat sources in closed objects. A re-projection scoring metric verifies accuracy; experiments demonstrate precise localization of invisible hot spots, making the method suitable for electrical-fault diagnostics. Souza [8] created "3D THERMO-SCAN," a multimodal medical-imaging workflow that integrates anatomical data from CT with infrared thermography, producing three-dimensional thermo-anatomical models for clinical analysis. Landmann [9] engineered a high-frame-rate 3-D thermographic sensor that couples GOBO structured-light profilometry with a long-wave-infrared (LWIR) high-speed camera, enabling simultaneous capture of object geometry and surface temperature. Liu's group [10] built a reflective laser-thermography inspection system for non-destructive characterization of micro-cracks on metallic surfaces. Adaptive Otsu thresholding accurately extracted crack contours, limiting area-measurement error to ≤25%. A temperature-field derivative-difference algorithm further constrained crack-depth estimation error to ≤7 %. He's team [11]

proposed Joint-Scanning Laser Thermography (JSLT), which combines line-laser synchronous scanning with a mid-wave-infrared (MWIR) camera to reconstruct temperature fields. Their column reconstruction–alignment–distortion correction algorithm expands the field-of-view 2.9-fold and doubles spatiotemporal resolution. On carbon-fiber-reinforced polymer panels, PCA/FFT post-processing reduced the detectable diameter-to-depth ratio to 3.33—achieving deeper and faster inspection than conventional pulsed thermography. Montinaro [12] validated Flying-Laser In-Probe Thermography (FLIPT) for in-situ inspection of additively manufactured metal parts. Finite-element transient-thermal analysis optimized laser power, region of interest, and scan speed; subsequent tests on Inconel 600 captured micron-scale porosity that matched simulations, demonstrating FLIPT's capability for real-time, non-contact quality assurance during metal AM.

Although extensive research has been devoted to a wide range of surface-inspection technologies, two-dimensional inspection of workpieces with complex profiles still faces formidable challenges. The pronounced geometric complexity of such profiles—multiple curved surfaces, deep recesses, and minute features—readily introduces projection distortion and local occlusion in 2-D imaging, leading to marked geometric discrepancies between infrared thermograms and visible-light images acquired from the same viewpoint. Moreover, because of the distinct physical characteristics of the two imaging modalities (for example, the lower spatial resolution of infrared thermography and the texture dependence of visible-light imaging), it is difficult to extract key contour features consistently across modalities, preventing high-precision, pixel-level registration between thermograms and visible-light images[13]. This cross-modal misregistration, driven by intricate geometric structures, severely limits the defect-detection accuracy achievable through multisource data fusion. To overcome this problem, this paper proposes a feasible method that relies solely on an infrared camera to perform both defect detection and three-dimensional reconstruction. By driving galvanometer mirrors at high speed, specific patterns (such as dot matrices or laser lines) are projected onto the specimen surface, enabling simultaneous defect detection and 3-D reconstruction and thereby offering a practical pathway to single-source three-dimensional thermography[14].

2. The principle and system of laser three-dimensional thermal imaging detection

2.1. Laser Centroid Detection and Subpixel Localization

Laser dot patterns typically appear as bright, roughly circular spots in the camera image. To ensure the accuracy of subsequent triangulation, the centroid for each spot must be provided at a subpixel level. In this paper, we employ a simple yet effective process of "adaptive thresholding + connected component extraction + grayscale centroiding." The steps and mathematical descriptions are as follows:

1.Grayscale Threshold Segmentation

Let the grayscale image be represented as I(x,y). Using Otsu's method or local adaptive thresholding, denoted as T, the laser spot is separated from the background, resulting in a binary mask[15]:

$$B(x,y)=\begin{cases}1, & I(x,y)\geq T\\ 0, & I(x,y)<T\end{cases} \tag{1}$$

2. Connected Component Filtering and Noise Removal

Perform an 8-neighborhood connected component analysis on B(x,y), retaining only the spots with an area in the range [Amin, Amax]. A morphological opening operation is then applied to exclude isolated noise and adjacent spots[16].

3. Grayscale Centroid Calculation

For each connected component R, calculate the first-order grayscale moment[17]:

$$M_{pq}=\sum_{(x,y)\in \mathrm{R}} x^{p}y^{q}I(x,y),\quad p,q\in\{0,1\} \tag{2}$$

The centroid coordinates are given by:

$$u_C=\frac{M_{10}}{M_{00}},\qquad v_C=\frac{M_{01}}{M_{00}} \tag{3}$$

where M00 represents the total grayscale intensity of the region, and (u_C, v_C) represents the subpixel laser centroid.

2.2. Laser Dot Grid-Based 3D Reconstruction Method

The laser dot grid structured light system consists of a projector and a camera. The projector casts a uniform laser grid onto the surface of the object, while the camera synchronously captures an image containing grid distortions. Let the optical centers of the camera and projector be denoted as O_C and O_P, respectively, with their intrinsic parameters represented as:

$$K_C=\begin{bmatrix}f_x & 0 & c_x\\ 0 & f_y & c_y\\ 0 & 0 & 1\end{bmatrix},\quad K_P=\begin{bmatrix}f_x' & 0 & c_x'\\ 0 & f_y' & c_y'\\ 0 & 0 & 1\end{bmatrix} \tag{4}$$

The extrinsic parameters of the projector (relative to the camera coordinate system) are denoted as (R_P, T_P). For a point (u_C, v_C) on the camera image plane and a point (u_P, v_P) on the projector image plane, homogeneous coordinates are constructed as follows:

$$\mathbf{p}_C = [u_C, v_C, 1]^T, \quad \mathbf{p}_P = [u_P, v_P, 1]^T \tag{5}$$

The back-projection yields the corresponding unit ray directions:

$$\mathbf{v}_C = \frac{K_C^{-1}\mathbf{p}_C}{\| K_C^{-1}\mathbf{p}_C \|}, \quad \mathbf{v}_P = R_P \left(\frac{K_P^{-1}\mathbf{p}_P}{\| K_P^{-1}\mathbf{p}_P \|} \right) \tag{6}$$

where v_C is the camera direction vector corresponding to the pixel (u_C, v_C), and v_P is the direction vector of pixel (u_P, v_P) transformed from the projector coordinate system to the world coordinate system.

The laser is emitted from the projector along v_P, and after being reflected by the surface of the object, it enters the camera along the v_C direction. Therefore, the laser point X simultaneously satisfies the constraints of the following two rays[18]:

$$\mathbf{X} = t \cdot \mathbf{v}_C, \quad \mathbf{X} = O_P + s \cdot \mathbf{v}_P, \quad t, s > 0 \tag{7}$$

By combining the two equations and eliminating X, we obtain:

$$A = [\mathbf{v}_C, -\mathbf{v}_P] \in \square^{3\times 2}, \quad \mathbf{b} = O_P \tag{8}$$

This can be formulated as an over-determined linear system:

$$A \begin{bmatrix} t \\ s \end{bmatrix} = \mathbf{b} \tag{9}$$

In an ideal noise-free scenario, v_C and v_P should intersect at point X. However, in practice, due to imaging errors or calibration inaccuracies, the two rays typically do not converge at a single point. Therefore, the least squares method is employed to find the parameters that minimize the distance between the rays[19]:

$$\begin{bmatrix} t^* \\ s^* \end{bmatrix} = A^{\dagger}\mathbf{b}, \quad \mathbf{X} = t^* \cdot \mathbf{v}_C \tag{10}$$

This process is repeated for each laser point, allowing the 3D reconstruction coordinates for all laser points to be obtained.

2.3. Laser Thermography Defect Detection Theory

Laser pulses heat the surface of a material, and the infrared thermography system records and analysis the temporal variation of surface temperature (thermal image sequence) to detect defects within or on the material surface, such as cracks, delamination, debonding, holes, and inclusions. The core theoretical foundation of this process is the unsteady-state heat conduction theory. The presence of defects alters the local thermophysical properties of the material (mainly thermal conductivity and heat capacity) or creates a thermal barrier, causing the heat flow to be obstructed at the defect site. This results in an abnormal "hotspot" pattern on the material's surface.

$$q = -k * \nabla T \tag{11}$$

The Fourier heat conduction law serves as the basis of heat conduction[20]. When a laser pulse heats the surface of the material, heat diffuses from the high-temperature region on the surface to the low-temperature region inside the material. If a defect (with low thermal conductivity) exists inside the material, the heat cannot be effectively conducted through the defect, leading to a slower temperature drop above the defect compared to the surrounding intact region.

$$\rho * c_p * \frac{\partial T}{\partial t} = \nabla \cdot (k * \nabla T) + Q \tag{12}$$

The heat-diffusion equation is the fundamental partial differential equation that governs the spatio-temporal evolution of the temperature field T(x,y,z,t) inside a material. Rooted in the law of energy conservation, it states that when a short laser pulse injects a large amount of thermal energy into the specimen surface—treated either as a boundary condition or as a near-surface volumetric heat source—the deposited heat subsequently diffuses through the bulk. According to the equation, the local rate of temperature rise equals the net heat flux entering the point plus any internal heat generation Q [21]. Subsurface defects perturb this diffusion process by locally altering the thermal conductivity k (and, in some cases, the density ρ and specific heat capacity c_p), thereby modifying the distribution of T(x,y,z,t). The resulting surface-temperature contrast at z = 0 is ultimately detected by the infrared thermal imager.

2.4. Three-Dimensional Laser Thermographic Inspection System

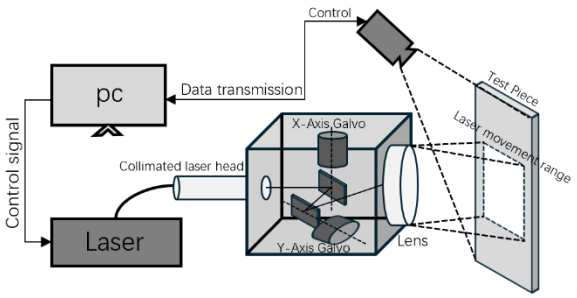

Fig. 1 *Three-Dimensional Laser Thermographic system*

The three-dimensional (3D) laser thermographic inspection system shown in Figure 1 is a non-contact, non-destructive testing (NDT) device based on the principle of active pulsed infrared thermography. It primarily consists of three components: a laser galvanometer system, an infrared thermographic acquisition system, and a data control and processing unit. The core working mechanism operates as follows: high energy-density laser dot arrays are used to actively excite the surface of the test object. At locations where internal defects (such as delaminations, voids, or inclusions) are present, the localized thermal diffusion behavior is disrupted. This anomaly alters the spatiotemporal evolution of the surface temperature field, making it possible to detect defect-induced thermal anomalies using an infrared camera, thus enabling defect identification. Simultaneously, the projected laser dot pattern on the component surface undergoes spatial distortion due to modulation by the micro- or macroscopic surface morphology. The infrared camera synchronously captures the spatial distribution characteristics of these morphology-modulated dot arrays, thereby facilitating the 3D reconstruction of the test object.

In this system, the laser source is guided via an optical fiber to a collimated laser head. Through high-speed oscillation of the laser galvanometer, arbitrary patterns (e.g., dot matrices or laser lines) can be generated on the object's surface. This allows for simultaneous heating and 3D reconstruction of the specimen[22]. The galvanometer system, based on the principle of reflection, dynamically controls the propagation direction of a single laser beam using rapidly deflecting mirrors. Compared to fixed optical components or mechanically driven platforms, the galvanometer offers superior scanning speed and positioning accuracy. It enables flexible and rapid guidance of the laser focus along arbitrary trajectories within a two-dimensional plane. This design allows the laser beam to scan large areas or complex paths at high speed and precision, significantly enhancing inspection or processing efficiency over static illumination or slow scanning approaches, while maintaining high spatial resolution and positioning accuracy[23]. Once laser excitation is complete, thermal diffusion occurs simultaneously. The entire temporal evolution of the surface temperature field is recorded by a high-frame-rate infrared thermal imager. This imager is synchronized with the laser trigger system to ensure accurate temporal alignment between temperature sampling and excitation. The multi-frame thermal images acquired by the infrared camera are transmitted via a high-speed data link to a computer, where a PC performs temperature data storage, preprocessing (such as non-uniformity correction and background temperature drift compensation), image analysis, and 3D reconstruction.

To enhance the visibility of potential subsurface anomalies, the post-processed thermal response is often logarithmically scaled to compress dynamic range and highlight subtle differences, which can be expressed as:

$$T_{\log}(x,y) = \log\left(\max_t T(x,y,t)\right) \tag{13}$$

Following this, a mild spatial Gaussian filter is applied to T_{log} to suppress noise and emphasize coherent thermal patterns across the surface, improving the signal-to-noise ratio for subsequent contrast operations.

To isolate regions exhibiting abnormal thermal behavior, the difference between the average thermal response and a scaled version of the logarithmic maximum is computed as:

$$\Delta T(x,y) = \left|\langle T(x,y,t)\rangle - \alpha \cdot T_{\log}(x,y)\right| \tag{14}$$

where ⟨T⟩ is the temporal average of temperature and α is an empirically chosen scaling factor (e.g., 0.7) that balances background suppression and anomaly enhancement.

Finally, to highlight sharp transitions associated with defect boundaries, a first-order spatial derivative is applied in the vertical direction:

$$\Delta T_y(x,y) = \left|\frac{\partial}{\partial y}\Delta T(x,y)\right| \tag{15}$$

This gradient map reveals localized temperature discontinuities, facilitating the detection and delineation of subsurface defects.

3. Results and Discussion

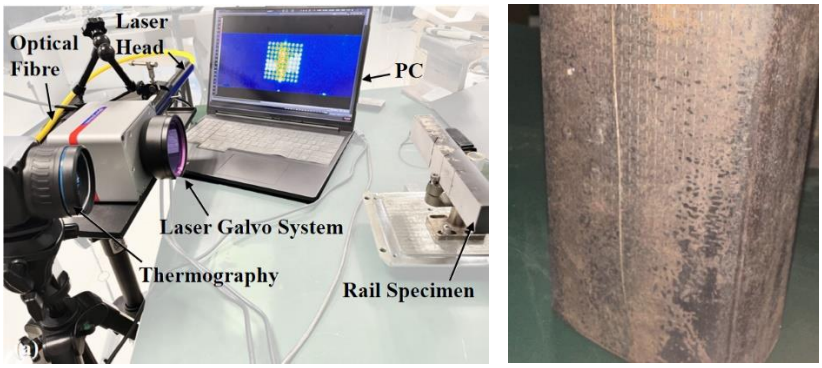

Fig. 2. *(a) Experimental setup (b) the steel rail specimen.*

Fig. 2(a) displays the experimental system for laser array scanning detection, which primarily consists of an infrared camera, a laser excitation system, a computer, and control equipment. The infrared camera used is the FLIR a655sc, which has a maximum sampling frame rate of F = 200 Hz, an integration time of less than 5 ms, and an image resolution of 640 × 480 pixels. This thermal imager is a high-performance model among uncooled thermal cameras, with a cost significantly lower than that of cooled thermal cameras. The excitation light source is a fiber laser with a single-point power P set to 2.46 W and a spot diameter w = 1 mm. The laser galvo system achieves fast and uniform laser movement through a motor-driven mirror. Fig. 2(b) illustrates the natural cracks on the rail tread, with a length almost passing through the test block and a width of 0.5mm.

We compared the following Conventional temporal features: Conventional temporal features: Principal Component Analysis (PCA) employs a low-dimensional mapping method, preserving the maximum diversity and retains the main components within the redundant data. When applied to thermal images, PCA often separate background and thermal target information in different components, and has effective enhancement and denoising effects. Independent Component Analysis (ICA) is similar to that of principal component analysis, with an additional requirement in the calculation process: the new coordinate system must be pairwise orthogonal, ensuring the decomposed signal components are independent of one another. In specific scenarios, ICA may outperform PCA in feature extraction [24]. Thermal signal reconstruction (TSR) performs N-order logarithmic fitting on the original data and obtains the partial derivatives respectively, which is characterized by improving the spatial and temporal resolution and amplifying the difference temperature changes with time. The reflection and occlusion information are effectively suppressed during the fitting process in this method. The process of pulse phase thermography analysis (PPT) is to perform Fourier transform on the thermal image sequence. The short pulse heating square wave signal encompasses multiple frequency components, providing valuable insights into the diffusion speed of thermal waves at various frequencies. This information proves instrumental in effectively detecting defects and determining their sizes, as well as discerning distinct material responses to thermal waves.

Method	PPT-Amplitude	PCA	ICA	TSR
Result	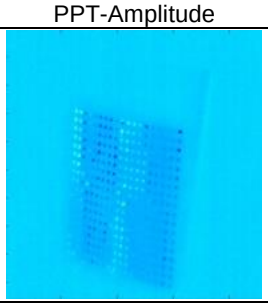			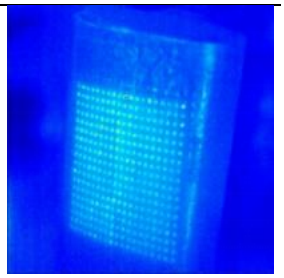
Method	PPT-Phase	Laser Spot Extraction	Proposed Method	3D result
Result	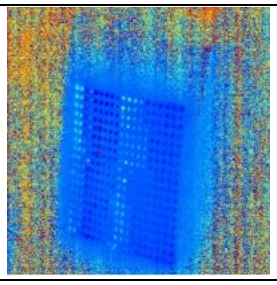	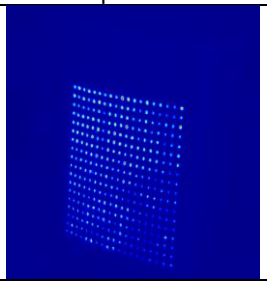	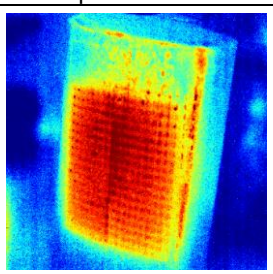	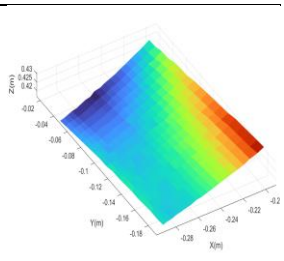

Fig. 3. *Comparison of experimental results of thermal sequence algorithm processing and three-dimensional reconstruction.*

Figure 3 shows all the comparative results and the results of the 3D reconstruction. It can be clearly seen from the figure that the conventional processing methods have significant problems in dealing with laser point interference, suffering from severe interference, which leads to inaccurate extraction of defect features. In contrast, the PCA and TSR processing results are relatively better and can effectively process and analyze the thermographic data to some extent, extracting more distinct defect features and demonstrating better performance. The ICA and PPT methods successfully extracted the amplitude and phase information and were able to capture the process of laser spots movement, providing certain basic data and feature information for subsequent analysis. However, in terms of suppressing laser point interference and highlighting defect features, they still have room for improvement compared with other methods.

The method proposed in this paper performs well in the comparison. It can accurately extract the position information of all laser points, which lays a solid foundation for subsequent processing steps. On the basis of accurately extracting the position of laser points, the method can also effectively remove the background interference of laser points to some extent, making the useful information in the thermographic data more prominent and facilitating further analysis. Moreover, the method can significantly enhance the temperature response of the crack defect in the middle, making the crack defect more distinctly visible in the thermographic data and greatly improving the detection sensitivity and accuracy of crack defects. In addition, the method successfully used the position of laser points to reconstruct the 3D profile of the rail surface, and the obtained 3D profile information has important application value. On the one hand, it can be used to identify certain specific defects, such as pits, coating blisters, and burrs. By analyzing the 3D profile, the presence and specific morphological characteristics of these defects can be accurately determined, providing a strong basis for defect diagnosis and evaluation. On the other hand, the 3D profile information can also be used for some profile measurement work and to achieve intuitive defect localization. In practical industrial inspection scenarios, this enables more precise identification of defect locations, providing accurate guidance for subsequent repair and treatment work, greatly improving work efficiency and quality, and offering an efficient and reliable solution for the surface inspection and defect identification of complex components, with certain industrial application prospects.

4. Conclusion

In this study, a novel three-dimensional laser thermographic inspection method was proposed to address the challenges of inspecting workpieces with complex profiles. The method relies solely on an infrared camera to perform both defect detection and three-dimensional reconstruction by projecting specific patterns onto the specimen surface. The results showed that the proposed method can accurately extract laser point positions, reduce background interference, enhance defect temperature response, and successfully reconstruct the three-dimensional profile of the rail surface. Compared to traditional methods, it demonstrated superior performance in defect detection accuracy. This method provides an effective solution for improving inspection accuracy and offers valuable profile information for defect recognition and localization, showing great potential for industrial applications. Future work will focus on further optimizing the algorithm and exploring more applications.

REFERENCES

[1] Qu Z, Jiang P, Zhang W. Development and application of infrared thermography non-destructive testing techniques[J]. Sensors, 2020, 20(14): 3851.
[2] Sutherland N, Marsh S, Priestnall G, et al. Infrared thermography and 3D-data fusion for architectural heritage: a scoping review[J]. Remote Sensing, 2023, 15(9): 2422.
[3] Akhloufi M A, Guyon Y, Castanedo C I, et al. Three-dimensional thermography for non-destructive testing and evaluation[J]. Quantitative InfraRed Thermography Journal, 2017, 14(1): 79-106.
[4] Gahleitner L, Mayr G, Burgholzer P, et al. Three-dimensional defect reconstruction in carbon fiber-reinforced composites with temporally non-uniform pulsed thermography data[J]. NDT & E International, 2025, 154: 103363.
[5] Özer Ö, Kumlutaş D, Yücekaya U A. A method for volumetric visualization of temperature distribution: three-dimensional meshed infrared thermography[J]. Experiments in Fluids, 2019, 60: 1-17.
[6] Heifetz A, Shribak D, Zhang X, et al. Thermal tomography 3D imaging of additively manufactured metallic structures[J]. AIP Advances, 2020, 10(10).
[7] Chen C Y, Yeh C H, Chang B R, et al. 3D reconstruction from IR thermal images and reprojective evaluations[J]. Mathematical Problems in Engineering, 2015, 2015(1): 520534.
[8] Abreu de Souza M, Alka Cordeiro D C, Oliveira J, et al. 3D multi-modality medical imaging: combining anatomical and infrared thermal images for 3D reconstruction[J]. Sensors, 2023, 23(3): 1610.
[9] Landmann M, Heist S, Dietrich P, et al. High-speed 3D thermography[J]. Optics and Lasers in Engineering, 2019, 121: 448-455.
[10] Liu J, Zhang Z, Lin Z, et al. Characterization method of surface crack based on laser thermography[J]. IEEE Access, 2021, 9: 76395-76402.
[11] He Z, Wang H, He Y, et al. Joint scanning laser thermography defect detection method for carbon fiber reinforced polymer[J]. IEEE Sensors Journal, 2019, 20(1): 328-336.

[12] Montinaro N, Cerniglia D, Pitarresi G. A numerical and experimental study through laser thermography for defect detection on metal additive manufactured parts[J]. Fracture and Structural Integrity, 2018, 12(43): 231-240.
[13] Jiang W, Pan H, Wang Y, et al. A multi-level cross-attention image registration method for visible and infrared small unmanned aerial vehicle targets via image style transfer[J]. Remote Sensing, 2024, 16(16): 2880.
[14] Xue, J.; Zhang, Q.; Li, C.; Lang, W.; Wang, M.; Hu, Y. *3D Face Profilometry Based on Galvanometer Scanner with Infrared Fringe Projection in High Speed.* Applied Sciences, 9 (7): 1458, 2019. DOI: 10.3390/app9071458.
[15] Li Y, Zhou J, Huang F, et al. Sub-pixel extraction of laser stripe center using an improved gray-gravity method[J]. Sensors, 2017, 17(4): 814.
[16] Kienle P, Nallar E, Köhler M H, et al. Analysis of sub-pixel laser spot detection in laser triangulation systems[C]//Optical Measurement Systems for Industrial Inspection XI. SPIE, 2019, 11056: 933-943.
[17] Cao J., Chen Y., Yu D., Xu Z., Hu X., *et al. Real-Time Laser Spot Detection and Tracking System Based on Parallel Multi-Target Detection and Determination Algorithm.* Review of Scientific Instruments, 94 (9): 095007, 2023. DOI: 10.1063/5.0157141.
[18] Ben-Hamadou A, Soussen C, Daul C, et al. Flexible calibration of structured-light systems projecting point patterns[J]. Computer Vision and Image Understanding, 2013, 117(10): 1468-1481.
[19] Tran V L, Lin H Y. A Structured Light RGB-D Camera System for Accurate Depth Measurement[J]. International Journal of Optics, 2018, 2018(1): 8659847.
[20] Usamentiaga R, Venegas P, Guerediaga J, et al. Infrared thermography for temperature measurement and non-destructive testing[J]. Sensors, 2014, 14(7): 12305-12348.
[21] Tomić L D, Jovanović D B, Karkalić R M, et al. Application of pulsed flash thermography method for specific defect estimation in aluminum[J]. Thermal Science, 2015, 19(5): 1845-1854.
[22] M. Belkacemi, C. Stolz, A. Mathieu, G. Lemaitre, O. Aubreton. *A combined three-dimensional digitisation and subsurface defect detection data using active infrared thermography.* Proc. QIRT 2016, 6 pp.
[23] Aubreton O, Bajard A, Verney B, et al. Infrared system for 3D scanning of metallic surfaces[J]. Machine vision and applications, 2013, 24: 1513-1524.
[24] Y. Wang, B. Gao, G. Tian, W. L. Woo, and Y. Miao, “Diffusion and separation mechanism of transient electromagnetic and thermal fields,” Int. J. Thermal Sci. vol. 02, pp. 308–318, 2016.